Meteoritics & Planetary Science 37, 311–327 (2002)
Available online at http://www.uark.edu/meteor

The irradiation history of the Ghubara (L5) regolith breccia

T. E. FERKO[1†], M-S. WANG[1], D. J. HILLEGONDS[1‡], M. E. LIPSCHUTZ[1*], R. HUTCHISON[2], L. FRANKE[3], P. SCHERER[3], L. SCHULTZ[3], P. H. BENOIT[4], D. W. G. SEARS[4], A. K. SINGHVI[5] AND N. BHANDARI[5]

[1]Department of Chemistry, Purdue University, West Lafayette, Indiana 47907, USA
[2]Department of Mineralogy, The Natural History Museum, Cromwell Road, London SW7 5BD, U.K.
[3]Max-Planck-Institut für Chemie, Postfach 3060, D-55020 Mainz, Germany
[4]Arkansas-Oklahoma Center for Space and Planetary Sciences, University of Arkansas, Fayetteville, Arkansas 72701, USA
[5]Physical Research Laboratory, Ahmedabad 380 009, India
†Present address: Department of Natural Science, California Baptist University, 8432 Magnolia Avenue, Riverside, California 92504, USA
‡Present address: Lawrence Livermore Laboratory, 7000 East Avenue, Livermore, California 94550, USA
*Correspondence author's e-mail address: rnaapuml@purdue.edu

(Received 2001 May 7; accepted in revised form 2001 November 16)

Abstract–We measured cosmic-ray products—noble gases, radionuclides, thermoluminescence, and nuclear tracks—and trace element contents and mineralogy of samples of three orthogonal and mutually intersecting cores (41–46 cm long) of a 101.6 kg Ghubara individual (1958,805) at The Natural History Museum, London. The xenoliths, like the host, have high concentrations of trapped solar gases and are heavily shocked. While contents of noble gases and degree of shock-loading in this individual and three others differ somewhat, the data indicate that Ghubara is a two-generation regolith breccia. Contents of cosmogenic ^{26}Al and ^{10}Be and low track densities indicate that the Ghubara individuals were located more than 15 cm below the surface of an 85 cm meteoroid. Because of its large size, Ghubara's cosmic-ray exposure age is poorly defined to be 15–20 Ma from cosmogenic nuclides. Ghubara's terrestrial age, based on ^{14}C data, is 2–3 ka. Not only is Ghubara the first known case of a two-generation regolith breccia on the macroscale, it also has a complicated thermal and irradiation history.

INTRODUCTION

As a meteoroid travels through space, cosmic rays interact with material in it producing a variety of markers including stable and radionuclides, tracks, and stored energy measurable by thermoluminescence (TL). The contents of cosmic-ray products in individual meteorites with simple irradiation histories vary with the preatmospheric size of the parent meteoroid, depth of samples, and/or target element composition. Over the past 30 years, many ordinary chondrites—such as St-Severin (Schultz and Signer, 1976), and the Madhipura, Udaipur, and Bansur trio (Bhattacharya *et al.*, 1980)—have been studied by using samples from a single drilled core in each (cf., Benoit and Chen, 1996, and references therein). Two intersecting perpendicular cores in Jilin (Heusser *et al.*, 1996) were studied and other researchers (*e.g.*, Graf *et al.*, 1990a, 1997; Sarafin *et al.*, 1985) have studied exposed surfaces of meteorites to obtain two-dimensional views of cosmic-ray product formation. Garrison *et al.* (1992) obtained a quasi-three-dimensional irradiation profile of Chico from short (3–6 cm) cores drilled in exposed surfaces and Wright *et al.* (1973) measured cosmogenic gases in three mutually perpendicular cores through the L6 chondrite Keyes. These data, laboratory irradiation experiments and related modeling (cf., Leya *et al.*, 2000) provide an understanding of cosmic-ray production in meteorites and have enhanced estimation of cosmic-ray exposure ages, preatmospheric sizes, and exposure histories.

Approximately 20% of H chondrites consist of light gray xenoliths set in darker chondritic hosts and presumably are regolith or fragmental breccias (Binns, 1968). A much smaller percentage of such breccias occur among L chondrites. Regolith breccias contain material irradiated to varying degrees on asteroid surfaces where significant amounts of solar noble gases and nuclear particle tracks accumulated through implantation of particles from the Sun. In this study, we obtained three complete orthogonal and mutually intersecting cores of Ghubara, a black xenolithic L5 chondrite (Binns, 1968), to better understand the three-dimensional relationship of cosmic-ray products such as noble gases, nuclear tracks, radionuclides, and TL in brecciated meteorites. Several large Ghubara individuals were found in Oman beginning in 1954 and have been described as internally fresh with only slightly weathered crust (Grady, 2000).

Prelude preprint MS#4543

EXPERIMENTAL PROCEDURES

Sampling

The primary goal of this study was to investigate systematic variations of cosmic-ray products and, so, we cored the largest Ghubara specimen, the 101.6 kg individual (1958,805) in the Natural History Museum (formerly British Museum (Natural History))—hereafter designated as BM 1958—which at the time represented nearly 50% of the recovered material. Several additional large individuals have since been recovered from the same site in Oman, although they are not listed by Grady (2000) or Koblitz (2000). For comparison with BM 1958 cores, we analyzed two samples of a fragment (hereafter referred to as MPI) temporarily at the Max-Planck Institut at Mainz and samples of two other individuals in the Natural History Museum's collection: a 16 kg stone, 1954,207 (BM 1954); and 1956,242 (BM 1956), a complete 27 kg specimen.

We prepared three orthogonal and mutually intersecting cores of BM 1958 at the Natural History Museum using a distilled-water-cooled ELH-110 volt DBIOEKL type 2 drill and a Marcrist 14 mm diamond crown bit corer. We documented the length and crossing position of each core relative to the others (Fig. 1). Cores A, B, and C (42.5, 45.8 and 41.2 cm long, respectively; Fig. 2), intersected at A24.5 cm, B18.0 cm, C22.9 cm numbered in the direction of the arrow in Fig. 1. Cores were cut in half lengthwise, half of each being stored for archival purposes. The other core halves were documented and sampled at Purdue University.

We examined cores visually, using descriptions of Binns (1968) to identify matrix and two xenolith types. Host material consists of loosely packed chondrules set in abundant dark matrix (Fig. 3). Xenolith type 1 (X1) is lighter in color with distinct, closely packed chondrules. Light-colored xenolith type 2 (X2) is less abundant but most easily discerned: it contains indistinct chondrules and has sharply defined boundaries with the host. We prepared detailed drawings showing surface material on both flat (sawed) and rounded sides of cores. From these drawings, we located samples for particular measurements.

We photographically documented both whole-core (Fig. 2) and 7 cm close-up sections (*e.g.*, Fig. 3) for a permanent record of sampling locations. We used appropriate illumination to accentuate metal grains to act as identification markers on sawn surfaces. Core A fragments were evenly spaced to show both individual pieces and the amount of material lost due to grinding during coring. Samples showing clean breaks (*e.g.*, B35.5 cm, Fig. 2) were juxtaposed. Additional spaces in cores B and C occurred where the three cores overlap. Since we could not determine grinding loss for individual fragments we assumed it to be uniform throughout each core, yielding a small

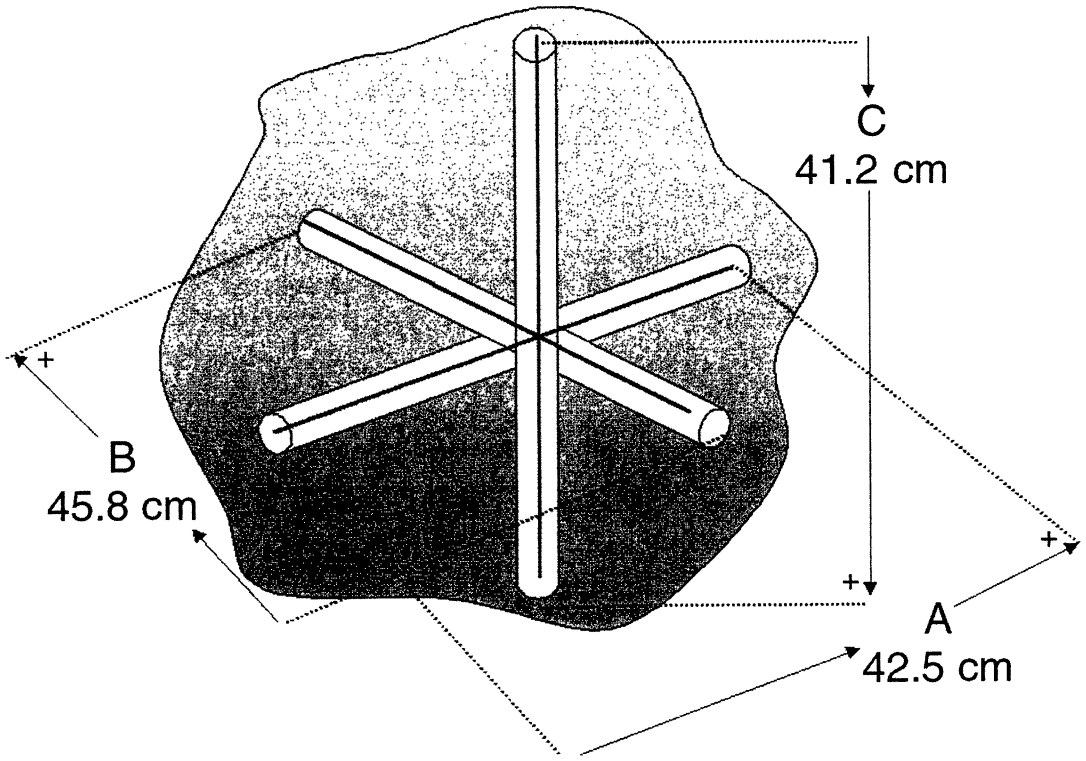

FIG. 1. Orientation and length of three orthogonal cores of the BM 1958 Ghubara stone. Each core is 1 cm in diameter and total lengths are indicated. Numbering for sample identification (cm) of each core progresses in the direction of the arrow: the intersection point is at (A24.5, B18.0, C22.9). The end of each core marked "+" in this and all similar figures denotes the highest sample number.

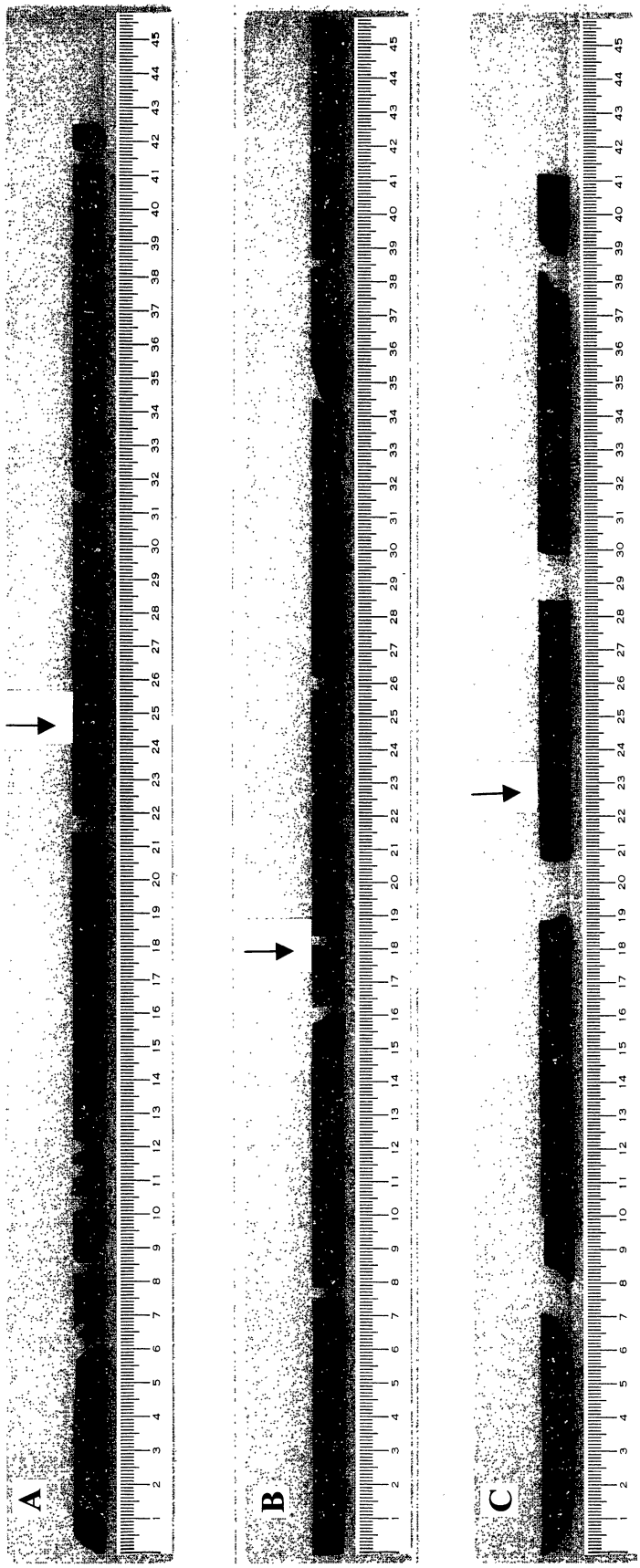

FIG. 2. Ghubara BM 1958 cores oriented as in Fig. 1. Shown are half of each core (cut lengthwise) with flat sides of individual fragments facing up. Fragments were spaced evenly in core A to show individuals and to account for loss due to grinding during coring. Additional space was allotted in cores B and C at the intersection point to account for material removed during drilling of the A core. The intersection point is marked by arrows (A24.5, B18.0, C22.9).

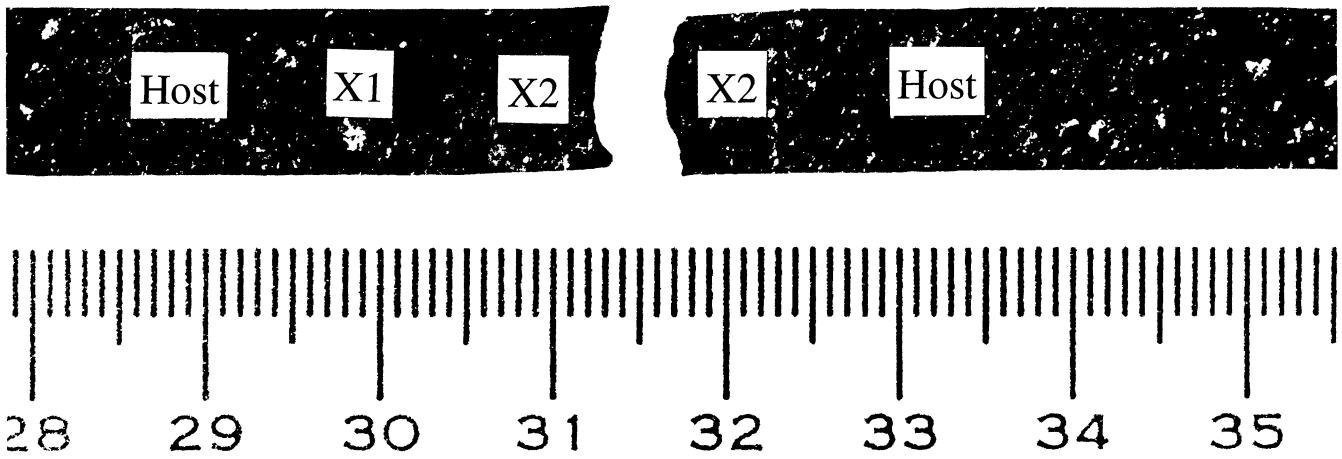

FIG. 3. A 7 cm close-up of Ghubara core A section showing host, xenolith 1 (X1), and xenolith 2 (X2). This is approximately centered on the second break from the right in core A (cf., Fig. 2).

uncertainty between the nominal and actual positions of samples in BM 1958.

The six end pieces (~0.8 to 3.2 cm in length) were either sampled by chisel or provided as complete fragments for nuclear track analysis. For other measurements, pieces of core fragments were separated and all exposed surfaces (core, sawed, and any oxidized material) were removed with a chisel. Where more than one type of material was present (host, X1 or X2), we sampled chips of each type. Samples for TL or radiochemical neutron activation analysis (RNAA) were weighed, crushed in an agate mortar, and separated into magnetic and non-magnetic (silicate) fractions. For TL, we analyzed only the silicate fraction: for RNAA, we reconstituted aliquots from three of these samples. When possible, we prepared homogenized samples of larger pieces (~1 cm) for noble gas and cosmogenic radionuclide studies by crushing them in an agate mortar to pass through 35 mesh teflon sieve. We separated metal and silicate fractions which were reconstituted for individual aliquots. Two samples (A10.6–11.2 cm and B13.3–13.6 cm) were not processed in this manner but were analyzed for noble gases as chips. In addition to the core samples, thin sections of BM 1958, BM 1954 and BM 1956 were prepared for petrographic study, and chips of BM 1954 were analyzed for noble gases and TL.

Noble Gases

Concentrations and isotopic composition of He, Ne, and Ar were measured in bulk samples of ~100 mg (Table 1) as described by Loeken *et al.* (1992). Uncertainties in the isotopic compositions are <1%, those of concentrations are estimated to be <5%. We calculated concentrations of cosmogenic ^{38}Ar and trapped ^{36}Ar using $(^{36}Ar/^{38}Ar)_c = 0.67$ and trapped $^{36}Ar/^{38}Ar = 5.32$. Cosmogenic ^{21}Ne was calculated assuming $(^{22}Ne/^{21}Ne)_c$ of 1.08 (see below) and solar $(^{22}Ne/^{21}Ne)_s = 32$.

Radionuclides

We measured ^{10}Be ($t_{1/2}$ = 1.50 Ma), ^{26}Al ($t_{1/2}$ = 705 ka), ^{36}Cl ($t_{1/2}$ = 301 ka) and ^{14}C ($t_{1/2}$ = 5.73 ka) by accelerator mass spectrometry (AMS) at Purdue University after having chemically separated the elements using previously published procedures (Vogt and Herpers, 1988; Jull *et al.*, 1989; Hillegonds, 2001). All $^{10}Be/^{9}Be$ ratios were measured relative to the PRIME Lab 5.000×10^{-12} standard, and increased by 17% to accommodate the discrepancy between NIST certified and AMS measured ratios (Vogt *et al.*, 1994). For converting $^{26}Al/^{27}Al$ ratios to ^{26}Al activities, we used the Al content of 1.23% measured in Ghubara host material by Binns (1968). To minimize chemical heterogeneity, all measurements were of BM 1958 host, except for a type 1 xenolith, A39.5–41.3 cm (Table 2). ^{14}C terrestrial age calculations (Table 3) follow those of Jull *et al.* (1989) with NIST SRM 4990C serving as primary ^{14}C standard.

Thermoluminescence

We measured TL at both the University of Arkansas (UA) (Table 4), and at the Physical Research Laboratory (PRL) (Table 5). At UA, measurements were performed on crushed samples using a 7.5 °C/s heating rate and an automated TL reader with Corning 7-59 and 4-69 filters and a EMI 9635 photomultiplier tube. For induced TL measurements, we irradiated samples with a $^{90}Sr/^{90}Y$ beta source with a ~20 Gy (Gray) (*i.e.*, 2 krad) dose. At PRL, TL was measured on HCl-cleaned samples of silicate fractions of BM 1954 and end pieces of cores A and C from BM 1958. Glow curves were obtained using a heating rate of 2 °C/s with an automated TL reader having Corning 7-59 + BG-39 filters coupled to an EMI 9835A bialkali photomultiplier tube. After recording the natural TL of the sample, the same aliquot was irradiated to 240 Gy

TABLE 1. Noble gas concentrations and ratios for Ghubara fragments.

Core	Type*	Noble gases†															
		^{3}He	^{4}He	^{20}Ne	^{21}Ne	^{22}Ne	^{36}Ar	^{38}Ar	^{40}Ar	$^{20}Ne/^{22}Ne$	$^{21}Ne/^{22}Ne$	$^{20}Ne_s$	$^{36}Ar_{trap}$	$^{3}He_c$	$^{21}Ne_c$	$^{38}Ar_c$	$(^{3}He/^{21}Ne)_c$
A2.6–3.0	X1	13.35	172	14.37	4.64	5.84	11.34	2.61	1544	2.46	0.795	10.2	11.0	13.35	4.62	0.55	2.89
A4.7–5.4	H	12.16	162	52.66	4.69	8.69	13.96	3.08	2000	6.06	0.540	48.5	13.6	12.16	4.57	0.52	2.66
A10.6–11.2	H	12.51	194	86.30	4.81	11.32	14.60	3.17	3044	7.62	0.425	82.1	14.3	12.51	4.61	0.49	2.71
A12.7–13.8	H	11.90	227	1108	7.53	92.99	60.89	11.89	2985	11.92	0.081	1104	60.5	11.90	4.79	0.51	2.48
A21.4–23.2	H	12.45	251	261.7	5.37	25.00	16.87	3.55	3442	10.47	0.215	257.4	16.6	12.45	4.75	0.43	2.62
A29.0–30.0	X1	12.71	286	405.0	5.85	36.09	20.20	4.22	4367	11.22	0.162	400.6	19.9	12.71	4.89	0.48	2.60
A31.7–32.4	X2	12.73	253	464.9	5.64	40.33	18.11	3.72	4708	11.53	0.140	460.8	17.9	12.73	4.53	0.36	2.81
A34.5–35.7	H	11.99	178	81.62	4.89	11.01	17.77	3.79	2644	7.41	0.444	77.3	17.4	11.99	4.70	0.51	2.55
A39.5–41.3	X1	13.00	254	20.33	4.21	5.77	7.37	1.84	696	3.52	0.730	16.5	7.0	13.00	4.17	0.52	3.11
B1.2–2.4	H	14.02	316	260.0	5.49	25.10	18.11	3.90	3187	10.36	0.219	255.6	17.7	14.02	4.87	0.57	2.88
B5.1–6.1	X2	14.48	404	490.0	6.53	43.26	15.24	3.29	4232	11.33	0.151	485.1	14.9	14.48	5.36	0.49	2.70
B10.8–12.3	H	13.17	260	257.7	5.48	24.75	16.38	3.49	2731	10.41	0.221	253.3	16.1	13.17	4.87	0.47	2.70
B13.3–13.6	H	10.34	179	260.4	5.29	24.86	23.91	4.90	3979	10.47	0.213	256.2	23.6	10.34	4.68	0.46	2.21
B15.3–15.8	X1	13.95	315	484.7	6.38	42.59	16.71	3.56	4421	11.38	0.150	480.0	16.4	13.95	5.23	0.48	2.67
B20.8–22	H	11.90	194	243.0	5.43	23.69	18.34	3.83	2573	10.26	0.229	238.6	18.0	11.90	4.85	0.44	2.45
B32.5–33.6	H	12.07	179	120.4	4.78	13.92	15.55	3.32	2908	8.65	0.343	116.3	15.2	12.07	4.50	0.45	2.68
B40.5–41.5	X1	12.67	185	321.0	5.69	30.07	47.08	9.21	3007	10.68	0.189	316.5	46.8	12.67	4.92	0.41	2.57
B41.6–42.6	H	10.66	160	206.2	4.42	19.99	16.92	3.56	3006	10.32	0.221	202.6	16.6	10.66	3.93	0.43	2.71
C4.2–5.5	H	11.28	157	76.9	4.37	10.20	11.77	2.59	2838	7.54	0.428	73.1	11.5	11.28	4.19	0.43	2.69
C13.3–14.7	H	11.87	160	83.34	4.30	10.58	13.26	2.89	2586	7.88	0.406	79.6	13.0	11.87	4.11	0.45	2.89
C25.8–26.4	X1	13.24	303	428.8	6.03	38.19	26.64	5.42	4708	11.23	0.158	424.3	26.3	13.24	5.01	0.47	2.64
C27.0–28.0	H	12.54	271	224.5	4.81	21.58	15.50	3.32	2670	10.40	0.223	220.6	15.2	12.54	4.27	0.47	2.93
C31.6–33.0	H	12.06	198	81.82	4.66	10.83	15.24	3.26	2665	7.55	0.430	77.8	14.9	12.06	4.47	0.45	2.69
C38.2–38.9	H	12.28	189	8.32	4.49	5.18	33.74	6.80	1763	1.61	0.867	4.3	33.4	12.28	4.48	0.52	2.74
1954,207	–	14.06	12860	1045	6.66	86.60	79.00	15.30	5060	12.07	0.077	1041.3	78.7	10.39	4.09	0.52	2.54
1956,242	–	15.91	20070	1022	6.51	83.75	54.58	10.69	4338	12.20	0.078	1018.0	54.2	10.18	4.03	0.49	2.53
MPI	X1	8.82	114	169.6	3.60	16.47	6.96	1.59	1991	10.30	0.219	166.7	6.7	8.79	3.20	0.32	2.75
MPI	H	8.09	106	149.6	3.99	15.46	13.12	2.75	2554	9.68	0.258	146.3	12.9	8.06	3.63	0.32	2.22

*Types of material are host (H), xenolith 1 (X1) and xenolith 2 (X2) from BM 1958 unless otherwise noted.
†Noble gas concentrations (units of 10^{-8} cm^3 STP/g) and $(^{3}He/^{21}Ne)_c$ ratios have uncertainties of <5%; $^{22}Ne/^{21}Ne$ ratio uncertainties are <1%.

TABLE 2. Cosmogenic radionuclide activities in Ghubara core samples.

Core/sampling distance*	^{10}Be† (dpm/kg)	^{26}Al† (dpm/kg)	^{36}Cl$_{metal}$† (dpm/kg)
A4.7–5.4	17.4 ± 0.4	58 ± 3	15.5 ± 0.5
A12.7–13.8	17.1 ± 0.4	62 ± 5	14.3 ± 0.5
A21.4–23.2	17.1 ± 0.4	63 ± 2	14.5 ± 0.5
A34.5–35.7	16.5 ± 0.3	57 ± 2	14.8 ± 0.6
A39.5–41.3	18.5 ± 0.4	58 ± 3	10.7 ± 0.4
B1.2–2.4	16.6 ± 0.4	60 ± 3	16.5 ± 0.6
B10.8–12.3	14.9 ± 0.5	64 ± 3	16.2 ± 0.5
B20.8–22.0	18.7 ± 0.5	61 ± 2	19.3 ± 0.6
B32.5–33.6	18.6 ± 0.6	59 ± 2	14.4 ± 0.7
B41.6–42.6	15.7 ± 0.7	57 ± 3	15.3 ± 0.6
C4.2–5.5	17.6 ± 0.8	59 ± 3	12.5 ± 0.5
C13.3–14.7	15.9 ± 0.7	61 ± 2	17.2 ± 0.7
C27.0–28.0	16.2 ± 0.7	57 ± 3	25.5 ± 0.9‡
C31.6–33.0	17.7 ± 0.7	60 ± 2	13.2 ± 0.6
C38.2–38.9	17.2 ± 0.7	59 ± 3	13.7 ± 0.5

*Sampling depth (cm) in the BM 1958,805 cores based on original notation.

†Uncertainties listed are ±1σ.

‡Small sample size and possible weighing error lead us to doubt the accuracy of this datum.

TABLE 3. ^{14}C contents and terrestrial ages of three Ghubara individuals.

Sample	^{14}C (dpm/kg)	Age (ka)*
BM 1958A13.8–14.4	37 ± 3	2.8 ± 1.4
BM 1958A5.7–6.0	38 ± 3	2.6 ± 1.4
BM 1954	39 ± 3	2.4 ± 1.4
BM 1956	39 ± 2	2.3 ± 1.3
Weighted mean	38 ± 1	2.5 ± 0.7

*Assuming 51 dpm/kg preterrestrial saturation activity for Bruderheim (Jull, pers. comm.).

with a ^{90}Sr/^{90}Y beta source and the TL was again recorded after a preheat of 250 °C for 1 min.

Nuclear Tracks

Selected grains and bulk grain mounts of the six end fragments of BM 1958 cores and a piece of BM 1954 were processed at PRL for nuclear track density measurements. Samples were etched with boiling WN etchant (*i.e.*, 40% EDTA, 1% oxalic acid and orthophosphoric acid adjusted to pH 8 by NaOH; Krishnaswami *et al.*, 1971) for 6 h (for olivines) and in boiling 1:1 NaOH for 1.5 h (for pyroxenes). Further etching (up to 10 h total) was found necessary for revealing some tracks in olivines (Table 6).

Radiochemical Neutron Activation Analysis

Sample and monitor preparation, irradiation conditions, chemical processing, and counting and data reduction

TABLE 4. Thermoluminescence in Ghubara cores.

Sampling depth	Type*	Natural TL (Eq Dose at 250 °C)	Sensitivity (Dhajala = 1)	TL peak width (°C)	TL peak (°C)
A2.5–3.2	X1	1.5 ± 0.2	0.76 ± 0.07	144 ± 2	200 ± 3
A5.4–5.8	H	4.0 ± 0.3	0.53 ± 0.04	142 ± 2	205 ± 4
A27.5–29.0	H	1.1 ± 0.2	0.57 ± 0.05	146 ± 1	206 ± 2
A28.9–30.2	X1	1.4 ± 0.2	0.68 ± 0.05	149 ± 2	212 ± 1
A30.5–31.5	X2	1.0 ± 0.3	0.90 ± 0.07	146 ± 1	203 ± 1
A37.3–37.8	H	0.9 ± 0.3	0.65 ± 0.02	146 ± 1	206 ± 5
A38.3–39.8	X1	2.8 ± 0.9	0.75 ± 0.02	143 ± 3	199 ± 1
B5.1–6.1	X2	1.3 ± 0.4	0.70 ± 0.04	148 ± 3	196 ± 3
B7.0–7.5	H	0.7 ± 0.2	0.64 ± 0.05	148 ± 3	212 ± 5
B13.7–14.5	H	0.5 ± 0.1	0.50 ± 0.02	141 ± 5	215 ± 1
B15.2–15.8	X1	1.0 ± 0.1	0.56 ± 0.02	145 ± 2	209 ± 6
B38.9–39.4	H	1.0 ± 0.4	0.39 ± 0.02	142 ± 7	205 ± 1
B40.5–41.5	X1	0.8 ± 0.1	0.69 ± 0.02	145 ± 3	201 ± 2
C16.4–17.3	H	0.7 ± 0.2	0.45 ± 0.03	148 ± 2	218 ± 3
C17.5–18.0	X1	0.7 ± 0.2	0.67 ± 0.04	148 ± 2	212 ± 4
C28.0–28.5	H	0.9 ± 0.4	0.53 ± 0.05	149 ± 3	213 ± 3
C25.8–26.4	X1	0.7 ± 0.3	0.60 ± 0.05	152 ± 3	211 ± 1

*Types of material are host (H), xenolith 1 (X1) and xenolith 2 (X2).

TABLE 5. Equivalent dose (Gy) estimates of Ghubara samples.*

Detection window	Glow curve (°C)	BM 1958 A0–1.2	BM 1958 C0–3.2	BM 1954
Blue	270	65	90	40
	310	390	620	290
	360	950	1580	820
U.V.	270	40	30	30
	310	310	270	280
	360	820	840	810

*The equivalent dose was measured on two aliquots of each sample by releasing the natural TL, then recording the induced TL for 240 Gy beta dose on the same specimen. Errors are estimated as ±20%.

TABLE 6. Track densities in Ghubara olivines.

Sample*	Track density (number of tracks) (cm^{-2})†	Track production rate (cm^{-2} Ma^{-1})	Shielding depth (cm)‡
A0–1.2	NT	–	>20
A41.7–42.5	NT	–	>20
B0–1.3	NT	–	>20
B44.0–45.8	4.5×10^4 (3)	6×10^3	14
C0-3.2	9×10^4 (3)	1.2×10^3	20
C39.2–41.2	7×10^4 (13)	1×10^4	12
BM 1954†	3.2×10^5 (19)	4.3×10^4	8

*First six samples are from BM 1958 cores while the last is from one fragment of BM 1954.
†"Ghost tracks" rather than true very heavy (VH) tracks.
‡Assuming Ghubara meteoroid radius of 85 cm.
NT = No tracks observed.

procedures were those routinely used in our laboratory (cf., Wolf and Lipschutz, 1995). We irradiated 100 mg samples for 2 days at the University of Missouri Research Reactor. Chemical yields were >30% for each element in the samples and >55% for each element in the monitors (Table 7).

RESULTS

Petrography

Older polished hand specimens and thin sections of BM 1954 and BM 1958 revealed subtle differences: metal grains in BM 1954 are larger while the troilite in BM 1958 is more frothy and porous. New thin sections of the three individuals also seem very similar: all three stones have a dusting of metal and sulfide droplets throughout the granular groundmass and the olivine composition is $Fo_{75.5\pm0.5}$. However, closer inspection indicates that BM 1954 experienced less shock than BM 1956 or BM 1958. Metal and troilite grains in BM 1958 occasionally show eutectic intergrowths indicative of residual temperatures ≥988 °C. Troilite is often spongy with included silicate, and metal and troilite have amoeboid outlines against granular silicates. Larger troilites in BM 1958 are sheared, with granular brecciated zones separating larger fragments. BM 1956 shows features similar to those of BM 1958, though not to the same degree. In contrast, troilite in BM 1954 is coarsely recrystallized but not spongy as in BM 1956 or BM 1958.

TABLE 7. Trace elements measured by RNAA.

	Ghubara (L5) BM 1958			Pantar I (H3-5)	
	H	X1	X2	D	L
Element	A27.5–29.0	A28.9–29.0	A30.5–31.2		
Au (ppb)	129	123	151	–	–
Co (ppm)	399	354	471	758	969
Sb (ppb)	120	64	63	–	–
Ga (ppm)	5.10	5.20	6.07	6.13	7.60
Rb (ppm)	5.47	2.68	3.62	3.58	2.89
Ag (ppb)	44.8	45.0	61.6	53.4	30.4
Se (ppm)	9.85	10.2	11.7	8.54	8.26
Cs (ppb)	182	217	387	248	60.5
Te (ppb)	426	551	560	643	298
Zn (ppm)	54.4	56.0	64.2	50.6	47.2
Cd (ppb)	15.9	6.34	7.53	21.8	6.97
Bi (ppb)	18.8	13.3	25.2	75.3	0.41
Tl (ppb)	12.0	10.3	10.5	31.6	0.55
In (ppb)	6.10	9.16	6.52	25.2	≤0.04

Types of material are host (H), xenolith 1 (X1) and xenolith 2 (X2) in Ghubara and dark (D) and light (L) in Pantar I (Lipschutz *et al.*, 1983).

Noble Gases

Five previous Ghubara noble gas analyses (Schultz and Franke, 2000) demonstrated high solar gas contents with ^{4}He of (3070–14 000) × 10^{-8} cm^3 STP/g and ^{20}Ne of (916–1100) × 10^{-8} cm^3 STP/g: these accord with our BM 1954 results (Table 1). One prior data set was made from material explicitly from the 1954 find (Vinogradov and Zadorozhnyi, 1965). Circumstantial evidence given in Levsky (1979) and Scherer (1993) imply that Ghubara samples studied by them also came from the 1954 find. These data contrast with those from BM 1958 core samples and the MPI samples which show significantly lower ^{4}He concentrations ((100–400) × 10^{-8} cm^3 STP/g)). While ^{4}He contents >2000 × 10^{-8} cm^3 STP/g in BM 1954 or BM 1956 are explained by the presence of trapped solar gas, the low values in BM 1958 may reflect loss by diffusion of radiogenic and/or solar ^{4}He caused by late thermal events.

A three-isotope plot of ^{20}Ne/^{22}Ne *vs.* ^{21}Ne/^{22}Ne (Fig. 4) shows the presence of trapped solar Ne throughout BM 1958. The data lie along a mixing line between solar and cosmogenic Ne. Using the regression line in Fig. 4 and assuming a cosmogenic ^{20}Ne/^{22}Ne ratio of 0.84, we calculate an average cosmogenic ^{22}Ne/^{21}Ne ratio of 1.08. The regression line drawn through BM 1958 samples and its intersection with the line connecting solar energetic particle (SEP) and solar wind (SW) Ne (Benkert *et al.*, 1988) indicates that solar Ne in Ghubara has a ^{20}Ne/^{22}Ne ratio of 12.9, typical of solar gas-containing chondritic breccias.

In typical regolith breccias, like Pantar, Fayetteville, Noblesville or Weston (König *et al.*, 1961; cf., Schultz and Franke, 2000), minerals of the light colored xenoliths were not irradiated by solar particles and thus do not contain trapped solar gases. In Ghubara BM 1958, however, light-colored xenoliths contain solar ^{20}Ne at concentrations higher than those of matrix samples. Since there is no evidence that this is due to matrix material adhering on the xenoliths, we infer that xenoliths themselves contain this significant characteristic of regolithic breccias and, thus, must be part of a second-generation regolith breccia from an earlier parent object. This is the second example of such an assemblage. Williams *et al.* (2000) described a single, equilibrated, microporphyritic impact

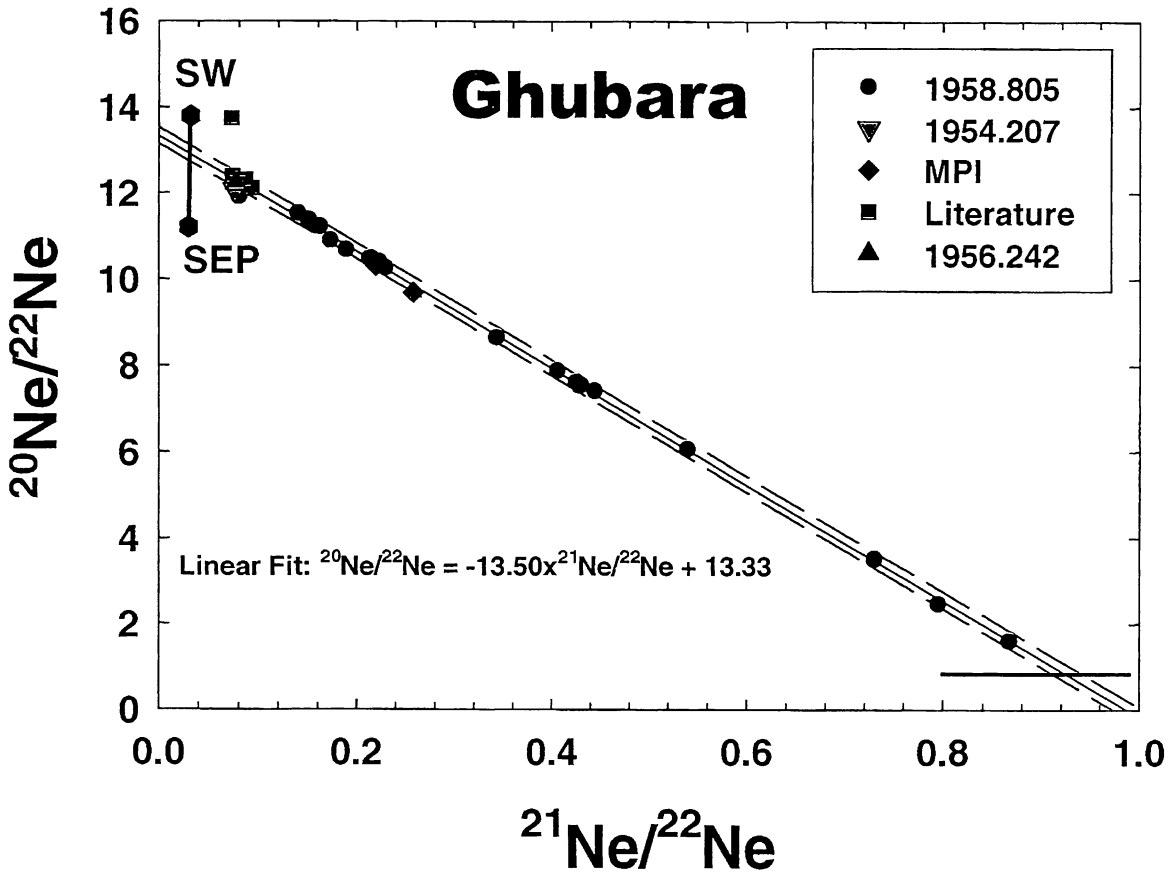

FIG. 4. Measured ^{21}Ne/^{22}Ne *vs.* ^{20}Ne/^{22}Ne for Ghubara samples. Data from this study are BM 1958 (circles), BM 1954 (inverted triangle), BM 1956 (triangle), and MPI (diamond). Literature data (squares) summarized by Schultz and Franke (2000) lie closest to the line connecting SW (solar wind) and SEP (solar energetic particles) with the datum from BM 1956 and one BM 1958 host sample, A12.7–13.8 (Table 1). All of the new data and all but one of the literature results accord well with the least-squares (continuous) line, whose equation is shown, as are the ±1σ (dashed) lines, connecting the pure cosmogenic production range (horizontal line at lower right) and solar component.

melt-rock clast within the H6 regolith breccia, Cangas de Onis. Whether that clast contains solar gases in unknown. In Ghubara, it is clear that each generation of regolith breccia generation is well represented.

Radionuclides

We list data for the three long-lived cosmogenic radionuclides in BM 1958 core samples in Table 2 and shorter-lived ^{14}C in Table 3. The ^{26}Al range of 57–64 dpm/kg, averaging 59.7 ± 2.2 dpm/kg, agrees with the average saturation value of 60 dpm/kg for L chondrites (Vogt *et al.*, 1990). However, the averages for ^{10}Be and metal-phase ^{36}Cl, 17.0 ± 1.1 and 15.5 ± 3.3 dpm/kg, respectively, fall below the corresponding average saturation values of 22.1 and 22.8 dpm/kg, respectively (Vogt *et al.*, 1990). No prior data for these radionuclides in Ghubara have been reported.

Thermoluminescence

Natural glow curves of samples of BM 1954 and cores A and C of BM 1958, show a near absence of low-temperature TL peak. Equivalent doses of the low-temperature and high-temperature peaks are about 0.5–5 Gy and 1000 Gy, respectively (Tables 4 and 5). For comparison, the corresponding values for the Dhajala chondrite are 600 and 1000 Gy. A progressive increase of equivalent dose with glow curve temperature suggests that the samples suffered either solar heating at a small perihelion distance of ~0.6 AU, or storage at elevated temperatures for some period. If Ghubara were a fresh fall, a low perihelion of ~0.6 AU and associated solar heating might be the preferred explanation (Benoit and Sears, 1997). However, since Ghubara has a terrestrial age of 2–3 ka and is a hot desert find, we attribute TL annealing to Ghubara's residence in a desert where surface temperatures of 60–70 °C are not uncommon. Meteorites with lower albedos could have attained even higher temperatures. Further, preservation of high-temperature TL also indicates that the Ghubara meteoroid's perihelion was ≥0.6 AU (Benoit *et al.*, 1991). The data for induced TL (sensitivity, peak width and peak temperature) are given in Table 4.

Tracks

Results of track density measurements are shown in Table 6. Even the near-surface grains of BM 1958 cores A and B do not show cosmic-ray tracks in either olivines or pyroxenes. Extended etching of olivines did reveal some track-like features in BM 1958 core C and BM 1954 but they do not appear fresh as are normally found in other meteorites and we refer to them as "ghost" tracks. From their appearance, they probably are not tracks of very heavy (VH) cosmic rays ($Z \approx 26$) formed during exposure of the meteoroid in interplanetary space. Data for pyroxenes are not included because pyroxenes in BM 1958 contain many bubbles and defects, precluding dependable track identification or counting.

Radiochemical Neutron Activation Analysis

Trace elements in adjacent samples of host, xenolith 1, and xenolith 2 are shown in Table 7. No prior data for these trace elements in Ghubara have been reported, although Binns (1968) indicated an order of magnitude estimate of 500 ppm Co obtained by electron microprobe, which is not greatly different from our mean value of 408 ppm (Table 7).

DISCUSSION

Regolith Exposure

Ordinary chondrite regolith breccias have two defining characteristics. First, they have a light-dark structure that results from inclusions (xenoliths) being set in a dark matrix (host) of smaller grains. This structure reflects "gardening" by repeated impacts on the surface of a body which comminutes surface materials into smaller fragments and mixes them over time. The host material is essentially fine-grained, comminuted rock while the xenoliths are rocklets with larger (millimeter to centimeter) sizes. Major element compositional differences between these materials are negligible (*e.g.*, Fredriksson and Keil, 1963; König, 1964).

During exposure on an asteroid surface, the second characteristic appears: solar particle tracks and implanted solar noble gases accumulate in fine-grained dust. Because of the particles' low energies, these solar irradiation effects are confined only to outer grain surfaces, <0.1 μm for noble gases and <0.1 cm for tracks (Caffee *et al.*, 1983). Cosmic-ray bombardment effects (*i.e.*, from high-energy (GeV) galactic cosmic rays (GCR)) penetrate to a meter or so. After exposure both on and near the surface, possibly including a period of deeper burial within the regolith, shock lithification of unconsolidated fragmented debris occurs, forming a regolith breccia (Bunch and Rajan, 1988). If deeply buried material is excavated by impact, it will again be exposed to GCR, perhaps as a meter-sized solid meteoroid which continues to accumulate irradiation effects. Thus, recovered regolith breccias contain a history of irradiation both in space (primarily galactic in origin) and in the parent body regolith (primarily, but not exclusively, solar in origin). Neutron effects indicative of deep burial in a parent body have been documented, for example, recently in the Fermo (H3-5) chondrite (Bonino *et al.*, 2001).

Clearly Ghubara is a regolith breccia since it has a classic light-dark pattern (Fig. 3) and shows distinct evidence for solar irradiation in its solar Ne (Fig. 4) with high $^{20}Ne/^{22}Ne$ ratios compared to cosmogenic neon. However, two other solar gas characteristics normally present in regolith breccias are absent in BM 1958: there is no difference in implanted solar gas concentrations between dark and light portions; and in the dark

portions, solar ^{4}He is not identifiable since most of the ^{4}He in them can be radiogenic. All regolith breccias studied previously show large solar Ne concentrations in dark matrix and little or none in light clasts (*e.g.*, Schultz and Signer, 1977; Wieler *et al.*, 1989a,b). While concentrations of solar neon vary in BM 1958, matrix and xenoliths show comparable ranges, with xenoliths tending to contain more solar ^{20}Ne (Table 1). The absence (probably loss) of solar ^{4}He from BM 1958 is apparent when it is compared with data from BM 1954/1956 (Table 1). Five previous Ghubara analyses, thought to be of BM 1954 (Schultz and Franke, 2000) and of BM 1956 show ^{4}He contents of (3070–20 000) × 10^{-8} cm^3 STP/g, a factor of 10 or more higher than those seen in BM 1958.

All three Ghubara individuals (BM 1954, BM 1956 and BM 1958)—and many other specimens—were found in Oman and it is tempting to attribute the different ^{4}He contents of BM 1954/1956 to BM 1958 being a unique and independent fall. However, other characteristics suggest that all individuals are from a single fall. All three BM individuals are petrographically similar: however, BM 1954/1956, which evidence less ^{4}He loss, are also less severely shocked (and heated) than BM 1958. All are regolith breccias, which are very rare among L chondrites: a search revealed only 16 L-chondrite regolith breccias, half of which are of petrographic type ≥4 (Koblitz, 2000; Schultz and Franke, 2000). Finally, all three have similar ^{14}C levels consistent with a terrestrial age of 2–3 ka (Table 3).

The Ne data for all three Ghubara individuals (including multiple samples of BM 1954/1956 and BM 1958) fall on a single three-isotope mixing line with very little scatter (Fig. 4). If BM 1954 represents a unique L-chondrite regolith breccia, its constituent end members are very similar to those of BM 1958. As seen in Table 8, cosmic-ray exposure ages based on ^{21}Ne and ^{38}Ar in BM 1954 and BM 1958 are also similar, indicating that these individuals derive from a single meteoroid, some part of which experienced lesser heating than the others. The fact that samples of BM 1954/1956 and BM 1958 have similar levels of ^{3}He suggests that any heating involving the Ghubara meteoroid occurred before its extended exposure to cosmic rays as a meter-sized object.

Since xenoliths in BM 1958 contain solar Ne at concentrations often exceeding those in the host (Table 1), it is likely that this Ghubara individual, at least, consists of ≥2 generations of regolith exposure. According to this scenario, these xenoliths represent lithified regolithic material from an earlier breccia that were mixed with present-day host in the Ghubara regolith. The resultant breccia (BM 1958) then experienced a heating episode sufficient to cause most of its solar and radiogenic ^{4}He to be lost, but not all solar Ne. This heating was localized since the Ghubara BM 1954/1956 individuals did not lose all of their ^{4}He. If such heating occurred on the parent body prior to the impact that sent the Ghubara meteoroid earthward, heated (BM 1958) and less heated (BM 1954) regions could have been ejected in the same event. Alternatively if the heating was shock-derived from the ejection event, shock-loading was anisotropic since BM 1954 was less heavily shock-affected, as observed petrographically.

TABLE 8. Noble gas exposure ages (Ma) of Ghubara.

Sample*	Type†	T^3He	T^{21}Ne	T^{38}Ar
A2.6–3.0	X	8.2	12.0	13.0
A4.7–5.4	H	7.5	11.9	12.4
A10.6–11.2	H	7.7	12.0	11.6
A12.7–13.8	H	7.3	12.5	12.1
A21.4–23.2	H	7.7	12.4	10.3
A29.0–30.0	X1	7.8	12.7	11.5
A31.7–32.4	X2	7.8	11.8	8.6
A34.5–35.7	H	7.4	12.3	12.2
A39.5–41.3	X1	8.0	10.9	12.4
B1.2–2.4	H	8.6	12.7	13.5
B5.1–6.1	X2	8.9	14.0	11.6
B10.8–12.3	H	8.1	12.7	11.2
B13.3–13.6	H	6.4	12.2	11.0
B15.3–15.8	X1	8.6	13.6	11.4
B20.8–22	H	7.3	12.6	10.4
B32.5–33.6	H	7.4	11.7	10.8
B40.5–41.5	X1	7.8	12.8	9.8
B41.6–42.6	H	6.6	10.2	10.3
C4.2–5.5	H	6.9	10.9	10.3
C13.3–14.7	H	7.3	10.7	10.8
C25.8–26.4	X1	8.1	13.0	11.2
C27.0–28.0	H	7.7	11.2	11.1
C31.6–33.0	H	7.4	11.7	10.8
C38.2–38.9	H	7.6	11.6	12.4
BM 1954	–	6.4	10.7	12.3
BM 1956	–	6.3	10.5	11.7
MPI	X	5.4	8.3	7.7
MPI	H	5.0	9.5	7.7

*BM1958 core samples unless otherwise noted.
†Types of material are host (H), xenolith 1 (X1), xenolith 2 (X2), or unclassified xenolith (X).

Localized heating such as that postulated for Ghubara BM 1958 is evident in properties other than the solar ^{4}He deficit. Regolith maturity can be estimated from induced TL (Haq *et al.*, 1989) which increases during repeated impacts and turnover. As regolith matures, concentrations of solar wind implanted elements and solar-flare particle tracks increase and the mean particle size, particularly of the host material, decreases (Bunch and Rajan, 1988). Such particle size changes, particularly in feldspar, affects TL sensitivity. In BM 1958 (Table 4), despite some overlap, host samples have lower TL sensitivity than xenolith samples (means of 0.53 ± 0.09 and 0.7 ± 0.1, respectively, relative to Dhajala) to yield a host/xenolith ratio near 0.8. The TL sensitivity ratio for ordinary

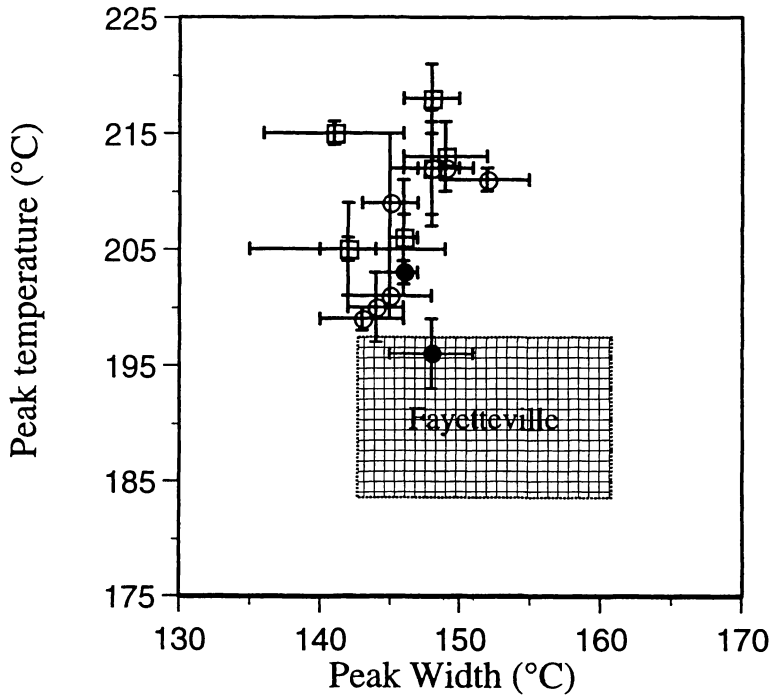

FIG. 5. Peak temperature *vs.* peak width for BM 1958 core samples as compared to the Fayetteville regolith breccia (rectangular region). Symbols denote host (open squares) and xenoliths (filled circles). The relatively large disparity between host and xenolithic samples from Ghubara indicates its relative immaturity.

chondrite regolith breccias varies from 1.0 (immature) to 0.1 (highly mature) in a log-linear fashion and correlates with other maturity indices, such as concentrations of volatile trace elements and carbon (Haq *et al.*, 1989). The TL sensitivity ratio for Ghubara near 0.8 indicates a rather immature regolith breccia, consistent with the similarities of the induced TL peak temperature and peak width data for clasts and matrix (Fig. 5).

RNAA data for labile trace elements also shed light on Ghubara's regolithic history. In H-chondrite regolith breccias, concentrations of highly volatile Bi, Tl and In vary with TL sensitivity ratio (Haq *et al.*, 1989). Pantar I (Lipschutz *et al.*, 1983), like Ghubara, has a sensitivity ratio near 0.8 and, to the extent that L- and H-chondrite regolith breccias behave similarly, we may compare their compositions (Table 7). In Pantar I, Bi, Tl and In contents are ~2 orders of magnitude higher in the dark matrix than in the light inclusions. Such differences are seen in essentially all H-chondrite regolith breccias. In contrast, Bi, Tl and In levels in Ghubara BM 1958 host are 20–40% of Pantar I dark, although they are similar to those in the BM 1958 xenoliths. This compositional similarity between host and xenoliths is consistent with the noble gas data and suggests that both materials are regolith breccias, albeit of different generations. The remaining RNAA data (Table 7) are less informative. Ghubara samples contain lesser quantities of siderophilic Co and Ga than Pantar I, in keeping with their chemical classes (L and H, respectively). Ghubara is rich in Rb and Cs: this is also a characteristic of H-chondrite regolith breccias (Lipschutz *et al.*, 1983). Concentrations of the next six elements in Table 7 (Ag to Zn) in Ghubara are similar to those in Pantar I dark. Low Cd contents in Ghubara may reflect this element's extraordinary mobility (ease of vaporization and loss) in even mildly heated chondrites (cf., Wang and Lipschutz, 1998).

Since there is considerable evidence that Ghubara BM 1958 experienced a transient heating event, possibly shock-induced, we should consider how this affected Ghubara's other properties, especially its noble gas contents. In "normal" (unheated) regolith breccias, solar gases are implanted during regolith exposure and at least partly retained during subsequent compaction into a coherent body. Thus, we expect that the correlation of solar gas contents would not depend on depth in such a meteoroid but that all solar implantation products would mutually correlate. To examine this, we show the $^{20}Ne/^{22}Ne$ and $^{21}Ne_c$ data as a function of core length (Fig. 6).

While ^{21}Ne varies only by about ±7% around a mean value of 4.68×10^{-8} cm^3 STP/g, the $^{20}Ne/^{22}Ne$ ratio is quite variable, lying between 2 and 12. Some interior samples of cores A and C have high $^{20}Ne/^{22}Ne$ ratios and this ratio is also high throughout core B, signaling the presence of gas-rich xenoliths. Low values on the outside might be explained by diffusive loss of some solar neon. Petrographic study reveals no evidence for terrestrial heating of the BM 1958 individual.

To examine shock-heating effects on noble gas contents, we compare data for BM 1958 with those in less-shocked BM 1954 (Table 1). Relative to Ghubara BM 1954 (*e.g.*, data summarized by Schultz and Franke, 2000), BM 1958 has lost relatively more ^4He than solar neon. Heating experiments on

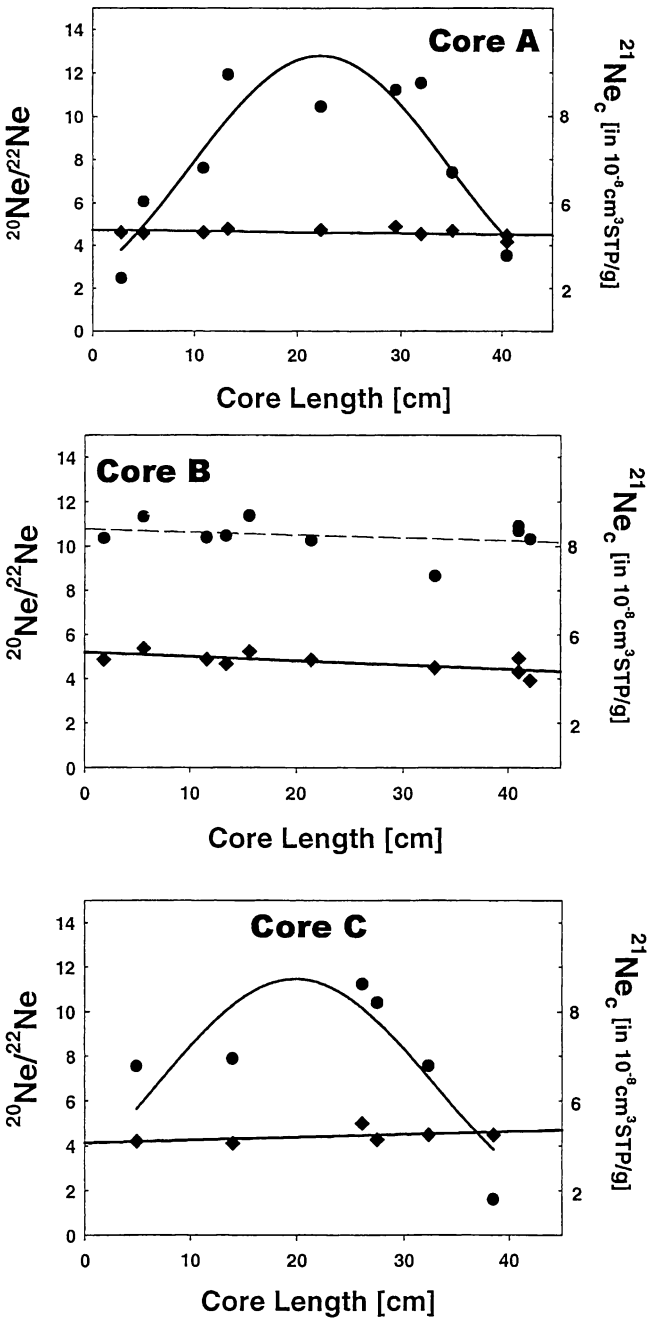

FIG. 6. The measured ratio of $^{20}Ne/^{22}Ne$, indicated by filled circles (left ordinate), and cosmogenic ^{21}Ne, indicated by filled diamonds (right ordinate), along the Ghubara BM 1958 cores. Possible profiles of the trends observed for $^{20}Ne/^{22}Ne$ are indicated. The $^{21}Ne_c$ curves in cores A and C are fit to an exponential function.

the solar gas-rich Kapoeta and Fayetteville (Black, 1972) reveal up to 90% ^4He loss, but only 70% of ^{20}Ne and ~40% of ^{36}Ar were lost by 350 °C. (In Allende, as well, He isotopes are readily lost relative to other noble gases as shown by their low apparent activation energies during simulated metamorphism; Herzog *et al.*, 1979.) Since Ghubara shows even greater gas loss, it may have been heated preterrestrially to >350 °C. The ^4He_s, which is most easily removed, indicates that BM 1958 was not isotropically degassed: the portion of the meteorite along the right side of the B axis must have been in a more insulated position since more ^4He was retained there than in other parts of the cores.

Other evidence for a heating episode following regolith exposure is provided by both induced TL and track data. TL peak temperature and width in chondrites are governed by thermal history (Haq *et al.*, 1989) and induced peaks tend to narrow and move to higher temperatures for severely annealed chondrites. For mature regoliths, the matrix exhibits broader peaks at lower peak temperatures compared to the clasts. Such effects are seen in BM 1958 (Fig. 5) with narrower peaks at higher temperatures compared to the best-documented, gas-rich regolith breccia, Fayetteville (Haq *et al.*, 1989).

Track data also indicate annealing. Nuclear track production rates in "normal" regoliths were significant and many breccias exhibit high track densities ($>10^7/cm^2$), steep gradients, and anisotropic orientation (Rajan, 1974). One grain of BM 1954 (Table 6) shows a track density of $\sim 3.4 \times 10^5/cm^2$ but it cannot be ascertained whether these are remnant solar flare tracks from regolith exposure or were formed during GCR exposure. In core end pieces from BM 1958, the upper limit of track density on two end pieces of core C is $\sim 10^4/cm^2$: no tracks were detected on the four end pieces of cores A and B. These densities are several orders of magnitude lower than expected for regolith exposure. Track annealing in both BM 1958 and BM 1954 indicates that both were heated to conditions high enough to remove tracks: however, in the latter, heating was less severe so that track and solar gas contents remained higher in that part of the meteoroid.

Exposure in the Parent Body

We follow Wieler *et al.* (1989a) in assigning the amounts of Ne in Ghubara introduced during regolith surface irradiation and by cosmic-ray exposure. While both sources contribute to ^{20}Ne and ^{21}Ne in Ghubara, the former is primarily solar while the latter is mainly cosmogenic. Ghubara matrix and xenolith contents of ^{21}Ne *vs.* ^{20}Ne roughly correlate (Fig. 7) and resemble the trend for Fayetteville matrix data (Wieler *et al.*, 1989a). We assume that such a trend implies exposure to energetic particles (whether T Tauri in origin (Caffee *et al.*, 1983) or cosmogenic (Wieler *et al.*, 1989a)) during the period in which solar Ne—mainly ^{20}Ne—accumulated in fine-grained regolith material.

From Fig. 7, $^{21}Ne = (4.4 \pm 0.3) \times 10^{-8}$ cm^3STP/g on the ordinate (at $^{20}Ne = 0$) for a best-fit line (having a slope of $314 \equiv (^{20}Ne/^{21}Ne)_s$) through the BM 1958 data points. Assuming $(^{20}Ne/^{22}Ne)_s = 12.9$ (Fig. 4), this yields a $(^{21}Ne/^{22}Ne)_s = 0.0417$. The corresponding $(^{22}Ne/^{21}Ne)_s = 24$, like that of Fayetteville, is considerably lower than the expected $(^{22}Ne/^{21}Ne)_s$ ratio (31.5 from Fig. 4). This suggests variations in the cosmogenic gas contents of individual samples.

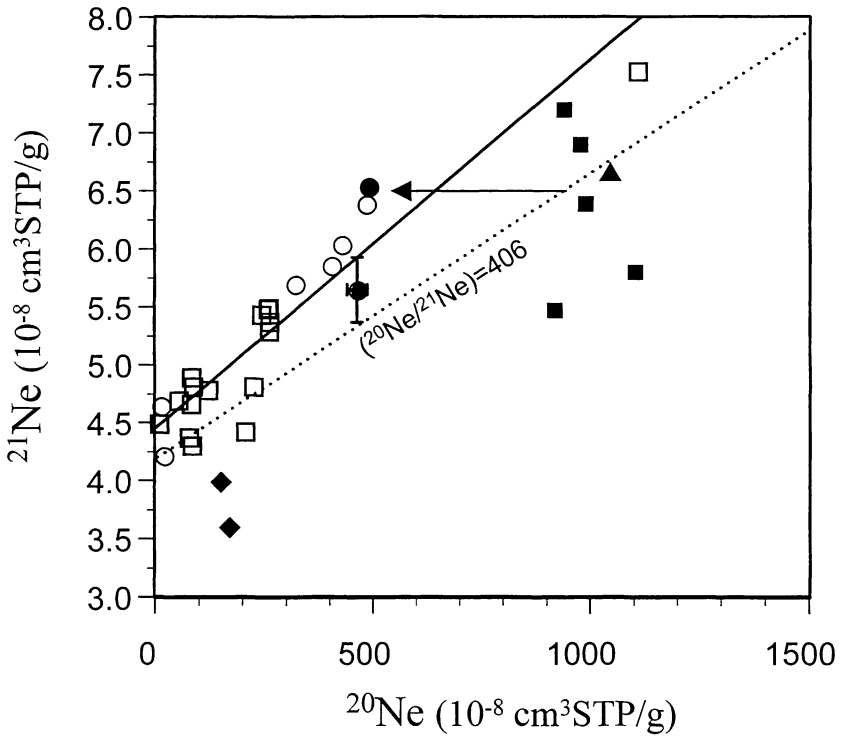

FIG. 7. Total ^{21}Ne *vs.* ^{20}Ne in Ghubara. The solid line is a best-fit line through BM 1958 core samples: host (open squares) and xenoliths (circles). The filled circle represents the most ^{4}He-rich sample in BM 1958 (B5.1–6.1 cm) while the open square in the upper right designates the most ^{20}Ne-rich sample (A12.7–13.8 cm). The closed triangle, squares and diamonds represent data for BM 1954, BM 1956 and MPI samples, respectively. The dotted line defines the ^{20}Ne/^{21}Ne mixing line obtained from the ^{20}Ne/^{22}Ne and ^{21}Ne/^{22}Ne relationship in Fig. 4. Higher levels of ^{21}Ne$_c$ are found in samples with higher ^{20}Ne$_s$ reflecting ^{20}Ne loss prior to build-up of ^{21}Ne$_c$ and/or accumulation of ^{21}Ne$_c$ during exposure in the regolith. While we favor the former explanation, the latter is not excluded by our data. The BM 1958 host sample, A12.7–13.8 cm, is as ^{20}Ne$_s$-rich as BM 1954 host samples (cf., Fig. 4). Regolith materials in the MPI sample had an implantation history different from other Ghubara samples. Representative uncertainties are shown for one datum.

However, while nearly all Fayetteville data fall on a ^{20}Ne/^{21}Ne line with slope = 303 (Wieler *et al.*, 1989a), Ghubara data scatter more. This, we take as additional evidence that irradiation episodes affecting Ghubara materials were more complex than those which produced "normal" regolith breccias like Fayetteville. Another (^{20}Ne/^{21}Ne)$_s$ line (with slope = 406) calculated from (^{20}Ne/^{22}Ne)$_s$ and (^{22}Ne/^{21}Ne)$_s$ ratios is included in Fig. 7 (cf., Fig. 4): this intercepts the ordinate at 4.2, corresponding to the least Ne-rich core sample (A39.5–41.3; Table 1). Two possible causes might account for the discrepant slopes: higher ^{21}Ne$_c$ from parent-body preirradiation in samples that contain higher ^{20}Ne$_s$ (as in Fayetteville) or preferential removal of the lighter ^{20}Ne isotope in a heating event (indicated by the arrow in Fig. 7) which would also account for spread in Ghubara data. Measurements of MPI and prior measurements of Ghubara 1954 (cf., Schultz and Franke, 2000) do not define the same line as BM 1958 (Fig. 7) supporting the notion of ^{20}Ne preferential removal but do not exclude the presence of preirradiation ^{21}Ne$_c$.

Schultz *et al.* (1971) found that in stepwise heating of lunar dust sample 10084 and two samples of the Weston regolith breccia, substantial proportions of solar ^{20}Ne were lost with ^{4}He at temperatures of 400–500 °C. In Ghubara BM 1958, concentrations of these two nuclides (and ^{20}Ne, ^{22}Ne and even the Ar isotopes) are substantially lower than the corresponding values in BM 1954 (Table 1; cf., Schultz and Franke, 2000).

Space Exposure

Radionuclides and Tracks–Activities of cosmogenic radionuclide levels allow us to estimate the radius of the Ghubara meteoroid during its last 5 Ma of cosmic-ray exposure. Using the radionuclide production estimates of Bhandari *et al.* (1993) and Leya *et al.* (2000), the ^{26}Al and ^{10}Be activity ranges of 57–64 and 14.9–18.7 dpm/kg, respectively (Table 2), indicate essentially constant saturation activities at depths >15 cm in an 85 cm object (Fig. 8). That the Ghubara meteoroid was so large is also supported by the average ^{26}Al/^{10}Be ratio in the cores, 3.5 ± 0.3. This corresponds well with the ratio of 3.42 ± 0.18 measured in Chico (Garrison *et al.*, 1992) which, in turn, accords with the ratio of 3.5 estimated at the center of large meteoroids (Leya *et al.*, 2000). Objects the size of Knyahinya and smaller exhibit ^{26}Al/^{10}Be ratios <3 (Graf *et al.*, 1990a).

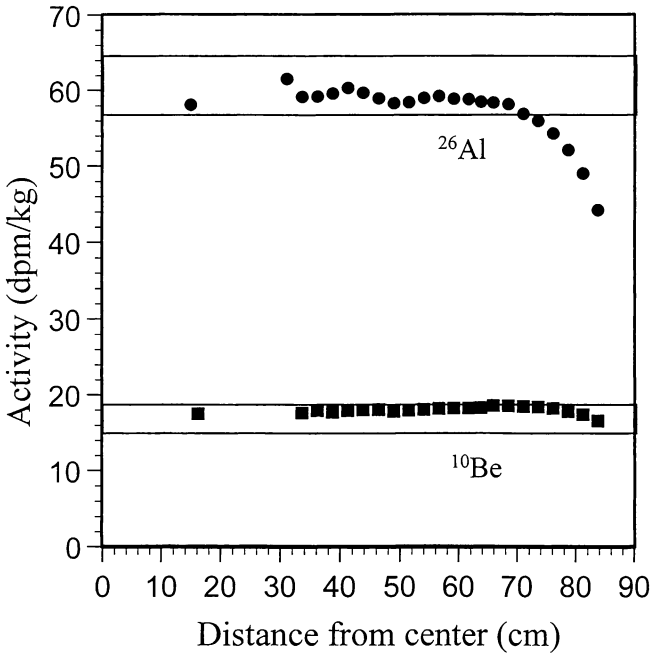

FIG. 8. Predictions of ^{26}Al (circles) and ^{10}Be (squares) contents in an 85 cm L chondrite of Ghubara's composition (Binns, 1968) from the model of Leya *et al.* (2000). ^{10}Be values are adjusted upward by 14% to account for an underestimation in the model (Leya *et al.*, 2000). Horizontal line pairs delineate the ranges of Ghubara data (Table 2).

Metal phase ^{36}Cl activities for an 85 cm chondrite with Ghubara's elemental composition (Binns, 1968) are predicted to range from 12 dpm/kg in the center to 17 dpm/kg at the surface (Leya *et al.*, 2000). This range is narrower than the range of 11 to 26 dpm/kg we measured in Ghubara (Table 2). Difficulties in weighing small metal masses (6–20 mg) free of adhering silicates may well be the reason for this discrepancy and we do not discuss these ^{36}Cl data further.

While the radionuclide data exhibit substantial scatter, plots of ^{26}Al and ^{21}Ne *vs.* depth show similar trends, especially in core A (Fig. 9). This suggests that some ^{26}Al variation is due to location in the parent meteoroid, supporting the notion that irradiation during the entire cosmic-ray exposure period (producing $^{21}Ne_c$) and during the last few million years (producing ^{26}Al) occurred under similar shielding. The ^{36}Cl depth profile (Fig. 10a) is consistent with that of ^{26}Al but the ^{10}Be depth profile (Fig. 10b) is different. Assuming a simple exposure during the last 5 Ma years, the ^{10}Be data seem to show larger uncertainties than those associated with the AMS measurements (Table 2). It would be useful to measure more depth-sensitive radionuclides (*i.e.*, ^{36}Cl in bulk and ^{26}Al in metal) to get further information about the meteoroid's exposure history. Fortunately, ample core materials remain and can be requested from The Natural History Museum.

Cosmic-Ray Exposure Age–Assuming a $(^{22}Ne/^{21}Ne)_c$ ratio of 1.08, average ^{10}Be/^{21}Ne and ^{26}Al/^{21}Ne exposure ages of 19 ± 2 and 16 ± 1 can be calculated (Graf *et al.*, 1990b).

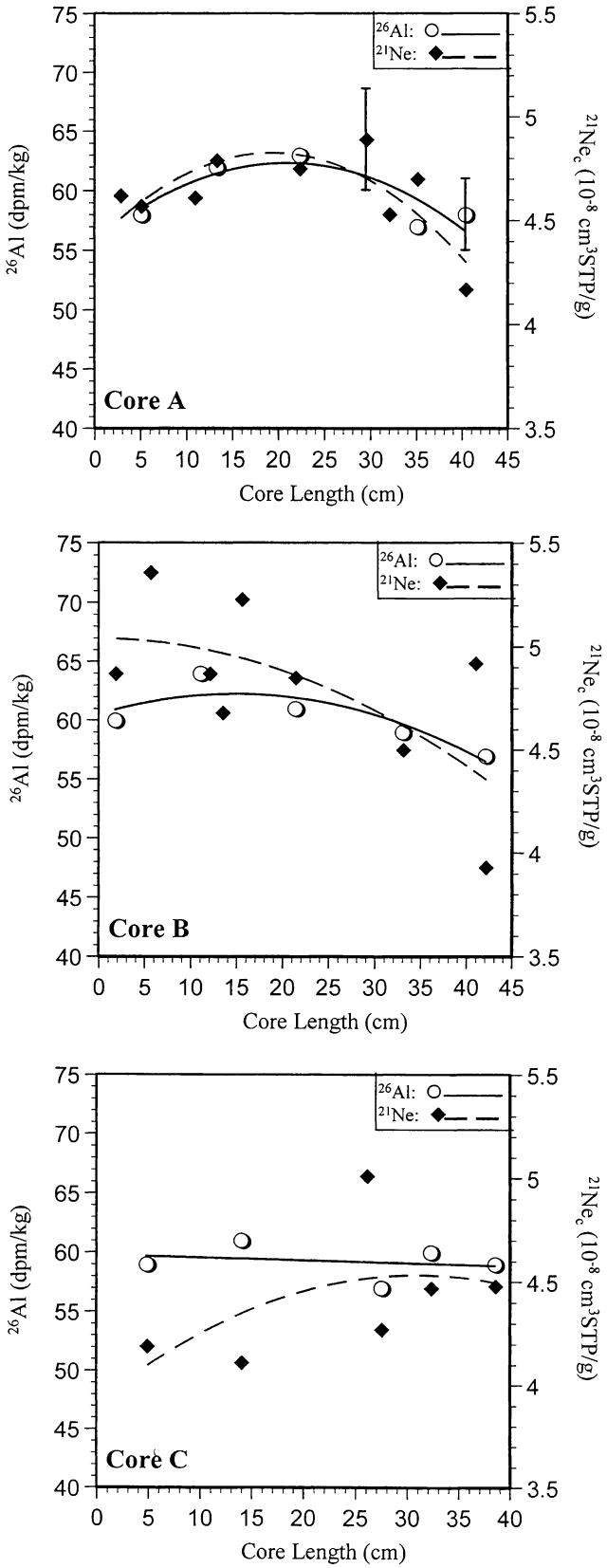

FIG. 9. Depth profiles of ^{26}Al and $^{21}Ne_c$ in Ghubara cores A, B, and C, respectively. Errors bars are shown for one representative datum each in panel A. Curves are fit to a quadratic equation.

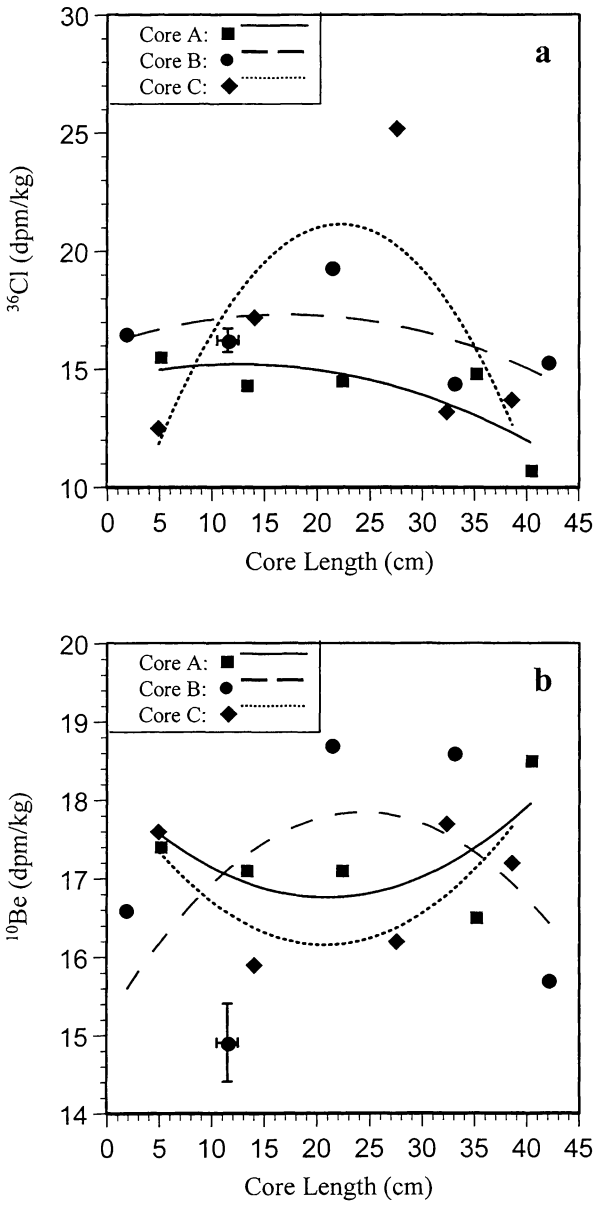

FIG. 10. Depth profiles of ^{36}Cl (a) and ^{10}Be (b) in Ghubara cores A, B, and C, respectively. Error bars are shown for one representative datum for each radionuclide. Curves are fit to a quadratic equation.

These cosmic-ray exposure ages disagree with the average ^{21}Ne age of 12 ± 1 Ma (Table 8) calculated using production rates of Eugster (1988) by >25% which is not surprising given the overestimated ^{21}Ne production rates in the Eugster (1988) formalism for high shielding, that is, ^{22}Ne/^{21}Ne < 1.09 (cf., Welten *et al.*, 2001). Conservatively, then, we conclude that Ghubara probably experienced a simple exposure in an 85 cm meteoroid during the last 15–20 Ma.

The measured track densities (1–33) × 10^4/cm^2 in olivines in ends of core C and in BM 1954 (Table 6) yields shielding depths of 12–20 cm for a 85 cm radius meteoroid if a 15 Ma cosmic-ray exposure age is assumed. For surface sample of cores A and B, we observed no tracks so that their shielding depths are probably larger. These shielding depths are consistent with the radionulide data discussed above.

Noble Gases–Assuming a 4π exposure age for BM 1958 of 15 Ma, ^{3}He$_c$, ^{21}Ne$_c$ and ^{38}Ar$_c$ produced at depths >15 cm in an 85 cm meteoroid would be approximately 21, 5 and 0.46 × 10^{-8} cm^3 STP/g, respectively (Wieler *et al.*, 1996; Leya *et al.*, 2000), comparable with the averages of 12.5, 4.6 and 0.5 × 10^{-8} cm^3 STP/g, respectively, found for Ghubara (Table 1).

^{3}He levels are rather constant in all Ghubara individuals (Table 1) but are comparatively low, resulting in low ^{3}He exposure ages (Table 8). This indicates that the meteoroid was thermally affected after ^{3}He production. ^{3}He loss is caused by solar heating at a small perihelion distance, which is also indicated by TL results. Such heating during a late stage in the history of the Ghubara meteoroid could also have affected the ^{4}He budget but this had already been influenced by shock heating, possibly during ejection of the Ghubara meteoroid. This heating was probably of short duration because not all parts of the Ghubara meteoroid (*e.g.*, BM 1954) exhibit the same amount of ^{4}He loss. Thus, the meteoroid was not thermally equilibrated. In this respect, Ghubara is unlike many other L chondrites which evidence more severe heating on the meter–kilometer scale generated during collisional breakup of their parent(s) 500–600 Ma ago. A scenario of mild, non-isotropic heating is consistent with the RNAA results. In most heavily shocked L chondrites, volatile trace elements can be lost to some extent (Walsh and Lipschutz, 1982; Huston and Lipschutz, 1984). However, samples of BM 1958 show high levels of volatile trace elements implying little, if any, heating loss.

Terrestrial History

Since Ghubara is a hot desert find, alteration by weathering could conceivably be problematic. Light noble gases (He, Ne and Ar) can be depleted in highly weathered specimens (Scherer *et al.*, 1994) with long terrestrial ages (Benoit *et al.*, 1993). However, hot desert finds have terrestrial ages of only several thousand years and show no noble gas depth correlation (Stelzner *et al.*, 1999). Ghubara shows little physical evidence of weathering (Grady, 2000) and terrestrial ages of Ghubara from all three individuals are 2–3 ka (Table 3): hence, weathering is unlikely to have caused >90% ^{4}He depletion in BM 1958 cores.

Terrestrial residence in a hot desert may, however, have caused low natural TL (NTL) levels. The NTL level at 250 °C in the glow curve is barely detectable. If Ghubara were a modern fall, we would interpret the data as indicating extensive solar heating, with a perihelion of ~0.6 AU (Benoit and Sears, 1997). The preservation of the high-temperature (400 °C) TL suggests that perihelion was not significantly less than this (Benoit *et al.*, 1991).

CONCLUSIONS

Ghubara is a regolith breccia exhibiting a light-dark structure each part of which contains solar gases. Based on induced TL sensitivity, its regolith was moderately mature, like Pantar I or St. Mesmin. While the three Ghubara individuals (BM 1954, 1956 and 1958) are mineralogically similar in general, there are noticeable differences, with BM 1954 showing less shock-loading than BM 1956 or BM 1958.

Differences between individuals are most noticeable for noble gases. BM 1958 cores have lost most of their solar ^{4}He compared with BM 1954/1956 and all previous Ghubara data. Heat-effects in BM 1958 are also evident in the loss of both low-temperature TL and nuclear tracks and in noble gas similarities between light and dark regions. Some loss of low-temperature TL might reflect Ghubara's residence in a hot desert for 2–3 ka but loss of nuclear tracks and noble gases would require higher temperatures. Since low-temperature TL is absent while high-temperature TL is still present, peak temperatures were <330 °C.

Our results indicate that Ghubara matrix and clasts represent two generations of asteroid regoliths where solar noble gases were implanted and cosmogenic noble gases were produced. This material was buried for times >4–5 Ma, then re-excavated and probably heated, perhaps by the impact that launched Ghubara earthward. The meteoroid acquired its cosmic-ray exposure age as an 85 cm meteoroid: some of the material (*i.e.*, most of BM 1958) was shielded at depths >30 cm. During the short heating, temperatures were non-uniform. Part of the object (now represented by BM 1958 and BM 1956—but not BM 1954) lost most or nearly all of the ^{4}He and nuclear tracks were erased from the BM 1958 precursor. Such heating differences are unprecedented in non-crater-forming events.

Acknowledgements–We are grateful to Bob Werberig for performing photographic documentation and to N. Sinha and K. M. Suthar for assistance in track analysis. Measurements at Purdue were supported by NSF grant 9510040-EAR and additional support was provided by NASA grant NAGW-3396 and Purdue University (National Need in Chemistry Fellowship to T. E. F.). We also thank Drs. K. Welten, in particular, and R. Wieler for incisive, thorough and provocative reviews of an earlier version of this paper. This work is in partial fulfillment of Ph.D. requirements for T. E. F. and D. J. H.

Editorial handling: I. C. Lyon

REFERENCES

BENKERT J-P., BAUR H., PEDRONI A., WIELER R. AND SIGNER P. (1988) Solar He, Ne, and Ar in regolith minerals: All are mixtures of two components (abstract). *Lunar Planet. Sci.* **19**, 59–60.

BENOIT P. H. AND CHEN Y. (1996) Galactic cosmic-ray-produced thermoluminescence profiles in meteorites, lunar samples, and a terrestrial analog. *Radiat. Meas.* **26**, 281–289.

BENOIT P. H. AND SEARS D. W. G. (1997) The orbits of meteorites from natural thermoluminescence. *Icarus* **125**, 281–287.

BENOIT P. H., SEARS D. W. G. AND MCKEEVER S. W. S. (1991) The natural thermoluminescence of meteorites II. Meteorite orbits and orbital evolution. *Icarus* **94**, 311–325.

BENOIT P. H., JULL A. J. T., MCKEEVER S. W. S. AND SEARS D. W. G. (1993) The natural thermoluminescence of meteorites VI: Carbon-14, thermoluminescence and the terrestrial ages of meteorites. *Meteoritics* **28**, 196–203.

BHANDARI N. *ET AL.* (1993) Depth and size dependence of cosmogenic radionuclide production rates in stony meteoroids. *Geochim. Cosmochim. Acta* **57**, 2361–2375.

BHATTACHARYA S. K., IMAMURA M., SINHA N. AND BHANDARI N. (1980) Depth and size dependence of ^{53}Mn activity in chondrites. *Earth Planet. Sci. Lett.* **30**, 191–199.

BINNS R. A. (1968) Cognate xenoliths in chondritic meteorites: Examples in Mezö-Madaras and Ghubara. *Geochim. Cosmochim. Acta* **32**, 299–317.

BLACK D. C. (1972) On the origins of trapped helium, neon and argon isotopic variations in meteorites–I. Gas-rich meteorites, lunar soil and breccia. *Geochim. Cosmochim. Acta* **36**, 347–375.

BONINO G., BHANDARI N., MURTY S. V. S., MAHAJAN R. R., SUTHAR K. M., SHUKLA A. D., SHUKLA P. N., CASTAGNOLI G. C. AND TARICCO G. (2001) Solar and galactic cosmic-ray records of the Fermo (H) chondrite regolith breccia. *Meteorit. Planet. Sci.* **36**, 831–839.

BUNCH T. E. AND RAJAN R. S. (1988) Meteorite regolith breccias. In *Meteorites and the Early Solar System* (eds. J. F. Kerridge and M. S. Matthews), pp. 144–164. Univ. Arizona Press, Tucson, Arizona, USA.

CAFFEE M. W., GOSWAMI J. N., HOHENBERG C. M. AND SWINDLE T. D. (1983) Cosmogenic neon from precompaction irradiation of Kapoeta and Murchison. *J. Geophys. Res.* **88**, B267–B273.

EUGSTER O. (1988) Cosmic-ray production rates for ^{3}He, ^{21}Ne, ^{38}Ar, ^{83}Kr, and ^{126}Xe in chondrites based on ^{81}Kr-Kr exposure ages. *Geochim. Cosmochim. Acta* **52**, 1649–1662.

FREDRIKSSON K. AND KEIL K. (1963) The light-dark structure in the Pantar and Kapoeta stone meteorites. *Geochim. Cosmochim. Acta* **27**, 717–739.

GARRISON D. H., BOGARD D. D., ALBRECHT A. A., VOGT S., HERZOG G. F., KLEIN J., FINK D., DEZFOULY-ARJOMANDY B. AND MIDDLETON R. (1992) Cosmogenic nuclides in core samples of the Chico L6 chondrite: Evidence for irradiation under high shielding. *Meteoritics* **27**, 371–381.

GRADY M. M. (2000) *Catalogue of Meteorites* (5th ed.). Cambridge Univ. Press, Cambridge, U.K. 689 pp.

GRAF T. *ET AL.* (1990a) Cosmogenic nuclides and nuclear tracks in the chondrite Knyahinya. *Geochim. Cosmochim. Acta* **54**, 2511–2520.

GRAF T., BAUR H. AND SIGNER P. (1990b) A model for the production of cosmogenic nuclides in chondrites. *Geochim. Cosmochim. Acta* **54**, 2521–2534.

GRAF T. *ET AL.* (1997) Exposure history of the Peekskill (H6) meteorite. *Meteorit. Planet. Sci.* **32**, 25–30.

HAQ M., HASAN F. A., SEARS D. W. G., MOORE C. B. AND LEWIS C. F. (1989) Thermoluminescence and the origin of the dark matrix of Fayetteville and similar meteorites. *Geochim. Cosmochim. Acta* **53**, 1435–1440.

HERZOG G. F., GIBSON E. K. AND LIPSCHUTZ M. E. (1979) Thermal metamorphism of primitive meteorites–VIII. Noble gases, carbon and sulfur in Allende (C3) meteorite heated at 400–1000 °C. *Geochim. Cosmochim. Acta* **43**, 395–404.

HEUSSER G., OUYANG Z., OEHM J. AND YI W. (1996) Aluminum-26, sodium-22 and cobalt-60 in two drill cores and some other samples of the Jilin chondrite. *Meteorit. Planet. Sci.* **31**, 657–665.

HILLEGONDS D. J. (2001) Radioçarbon applications in cosmochemistry and biomedical tracing. Ph.D. thesis, Purdue University, West Lafayette, Indiana, USA. 117 pp.

HUSTON T. J. AND LIPSCHUTZ M. E. (1984) Chemical studies of L chondrites–III. Mobile trace elements and ^{40}Ar/^{39}Ar ages. *Geochim. Cosmochim. Acta* **48**, 1319–1329.

JULL A. J. T., DONAHUE D. J. AND LINICK T. W. (1989) Carbon-14 activities in recently fallen meteorites and Antarctic meteorites. *Geochim. Cosmochim. Acta* **53**, 2095–2100.

KOBLITZ J. (2000) *Metbase 5.0*. Meteorite Data Retrieval Software, Fischerhude, Germany (CD-ROM).

KÖNIG H. (1964) Die chemische Zusammensetzung der hellen und dunklen Anteile des Meteoriten Pantar. *Geochim. Cosmochim. Acta* **28**, 1397–1399.

KÖNIG H., KEIL K., HINTENBERGER H., WLOTZKA F. AND BEGEMANN F. (1961) Untersuchungen an Steinmeteoriten mit extrem hohen Edelgasgehalt, I. Der Chondrit Pantar. *Z. Naturf.* **16A**, 1124–1130.

KRISHNASWAMI S., LAL D., PRABHU N. AND TAMHANE A. S. (1971) Olivines: Revelation of tracks of charged particles. *Science* **174**, 287–291.

LEVSKY L. K. (1979) Redkiye gazi v uglistkikh kondritakh (Noble gases in carbonaceous chondrites.) *Meteoritika* **38**, 27–36.

LEYA I., LANGE H-J., NEUMANN S., WIELER R. AND MICHEL R. (2000) The production of cosmogenic nuclides in stony meteoroids by galactic cosmic-ray particles. *Meteorit. Planet. Sci.* **35**, 259–286.

LIPSCHUTZ M. E., BISWAS S. AND MCSWEEN H. Y., JR. (1983) Chemical characteristics and origin of H chondrite regolith breccias. *Geochim. Cosmochim. Acta* **47**, 169–179.

LOEKEN T., SCHERER P., WEBER H. W. AND SCHULTZ L. (1992) Noble gases in 18 stone meteorites. *Chem. Erde* **52**, 249–259.

RAJAN R. S. (1974) On the irradiation history and origin of gas-rich meteorites. *Geochim. Cosmochim. Acta* **38**, 777–788.

SARAFIN R., BOUROT-DENISE M., CROZAZ G., HERPERS U., PELLAS P., SCHULTZ L. AND WEBER H. W. (1985) Cosmic-ray effects in the Antarctic meteorite Allan Hills A78084. *Earth Planet. Sci. Lett.* **73**, 171–182.

SCHERER P. (1993) Einfluss der terrestrischen Verwitterung auf den Edelgasgehalt und die Petrographie von Meteoriten; vergleichende Analysen von Chondriten aus polaren und subtropischen Trockenregionen. Ph.D. thesis, Johannes Gutenberg-Universität Mainz, Germany. 189 pp.

SCHERER P., SCHULTZ L. AND LOEKEN T. (1994) Weathering and atmospheric noble gases in chondrites. In *Noble Gas Geochemistry and Cosmochemistry* (ed. J. Matsuda), pp. 43–53. Terra Scientific Publishing Company, Tokyo, Japan.

SCHULTZ L. AND FRANKE L. (2000) *Helium, Neon, and Argon in Meteorites—A Data Compilation.* Update 2000. Max-Planck-Institut für Chemie, Mainz, Germany (CD-ROM).

SCHULTZ L. AND SIGNER P. (1976) Depth dependence of spallogenic helium, neon, and argon in the St-Severin chondrite. *Earth Planet. Sci. Lett.* **30**, 191–199.

SCHULTZ L. AND SIGNER P. (1977) Noble gases in the St. Mesmin chondrite: Implications to the irradiation history of a brecciated chondrite. *Earth Planet. Sci. Lett.* **36**, 363–371.

SCHULTZ L., FRICK U. AND SIGNER P. (1971) Nachweis des Diffusionsverlustes von Sonnenwind-^{4}He im Mondstaub. *Helv. Phys. Acta* **44**, 614–617.

STELZNER T. *ET AL.* (1999) An interdisciplinary study of weathering effects in ordinary chondrites from the Acfer region, Algeria. *Meteorit. Planet. Sci.* **34**, 787–794.

VINOGRADOV A. P. AND ZADOROZHNYI I. K. (1965) Kozmogenniye, radiogenniye i pervichniye inertniye gazi v kamennikh meteoritakh. (Cosmogenic, radiogenic and primordial inert gases in stone meteorites.) *Meteoritika* **26**, 77–90.

VOGT S. AND HERPERS U. (1988) Radiochemical separation techniques for the determination of long-lived radionuclides in meteorites by means of accelerator-mass-spectrometry. *Fresenius Z. Anal. Chem.* **331**, 186–188.

VOGT S., HERZOG G. F. AND REEDY R. C. (1990) Cosmogenic nuclides in extraterrestrial materials. *Rev. Geophys.* **28**, 253–275.

VOGT S., WANG M-S., LI R. AND LIPSCHUTZ M. (1994) Chemistry operations at Purdue's Accelerator Mass Spectrometry Facility. *Nucl. Instrum. Methods Phys. Res.* **B92**, 153–157.

WALSH T. M. AND LIPSCHUTZ M. E. (1982) Chemical studies of L chondrites–II. Shock-induced trace element mobilization. *Geochim. Cosmochim. Acta* **46**, 2491–2500.

WANG M-S. AND LIPSCHUTZ M. E. (1998) Thermally metamorphosed carbonaceous chondrites from data for thermally mobile trace elements. *Meteorit. Planet. Sci.* **33**, 1297–1302.

WELTEN K. C., NISHIIZUMI K., MASARIK J., CAFFEE M. W., JULL A. T. J., KLANDRUD S. E. AND WIELER R. (2001) Cosmic-ray exposure history of two Frontier Mountain H-chondrite showers from spallation and neutron-capture products. *Meteorit. Planet. Sci.* **36**, 301–317.

WIELER R., BAUR H., PEDRONI A., SIGNER P. AND PELLAS P. (1989a) Exposure history of the regolith chondrite Fayetteville: I. Solar-gas-rich matrix. *Geochim. Cosmochim. Acta* **53**, 1441–1448.

WIELER R. *ET AL.* (1989b) Exposure history of the regolith chondrite Fayetteville: II. Solar-gas-free light inclusions. *Geochim. Cosmochim. Acta* **53**, 1449–1459.

WIELER R. *ET AL.* (1996) Exposure history of the Torino meteorite. *Meteorit. Planet. Sci.* **31**, 265–272.

WILLIAMS C. V., KEIL K. AND TAYLOR G. J. (2000) Breccia within breccia in the Cangas de Onis regolith breccia: Implications for the history of the H chondrite parent body regolith. *Chem. Erde* **60**, 269–277.

WOLF S. AND LIPSCHUTZ M. E. (1995) Chemical studies of H chondrites. 6. Antarctic/non-Antarctic compositional differences revisited. *J. Geophys. Res.* **100**, 3335–3349.

WRIGHT R. J., SIMMS L. A., REYNOLDS M. A. AND BOGARD D. D. (1973) Depth variations of cosmogenic noble gases in the ~120 kg Keyes chondrite. *J. Geophys. Res.* **78**, 1308–1318.